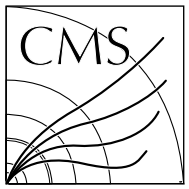

The Compact Muon Solenoid Experiment

CMS Note

Mailing address: CMS CERN, CH-1211 GENEVA 23, Switzerland

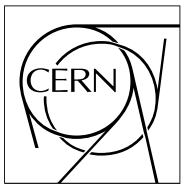

22 May 2006

Little Higgs Model and Top-like Heavy Quark at CMS

K. Karafasoulis, A. Kyriakis, H. Petrakou

Institute of Nuclear Physics,NCSR "Demokritos", Athens, Greece

K. Mazumdar

EHEP Group, Tata Institute of Fundamental Research, Mumbai, India.

Abstract

The *Little Higgs* model gives an alternative solution to the fine-tuning problem present in the Standard Model (SM) of strong and electroweak interactions. The model invokes several new particles of TeV mass range, the lightest among them being a heavy quark (T) of charge +2/3. The CMS potential to discover this particle during intial years of LHC running is investigated.

1 Introduction

Most extensions of the Standard Model (SM) contains extended gauge sector and/or extended Higgs sector but they are severely constrained by precision electroweak data. Any new physics at TeV scale has to be weakly coupled. The SM has passed stringent experimental verifications up to the electroweak scale ($\sim$ 200 GeV). If radiative corrections to the Higgs boson mass are computed using an ultra-violet cut off Λ, the resulting value of the Higgs boson mass is of $\mathcal{O}$ (Λ) unless very fine tuning and delicate cancellations take place. The precision measurements however indicate that the physical mass of the Higgs boson is $\leq$ 207 GeV/c^2 at 95% CL (Ref. [1]).

The *Little Higgs* model (Ref. [2]) provides just enough new physics to generate cancellations and preserve a light Higgs boson while raising the ultra-violet cut off to a scale of several tens of TeV where constraints of new particles from existing experiments are very weak. The gap between electroweak scale and this cutoff value is called the 'little hierarchy'.

The hierarchy problem is solved in the *Little Higgs* model by requiring the mass of the SM Higgs boson, $m_{\rm h}$, to be safe from only one-loop divergences. Thus Higgs boson mass is parametrically 2-loop factors smaller than Λ, instead of one. The SM is considered as part of a larger symmetry group. In the minimal scenario, both gauge and Yukawa interactions are necessary to break all the global symmetry which protect the Higgs boson mass. As a consequene, new particles are invoked whose couplings are sufficiently adjusted to cancel the large contribution of the SM particles to the Higgs boson mass. These additional particles are (Ref. [3]):

- A new heavy, singlet quark of charge 2/3: **T**.
- New heavy gauge bosons: $\rm W_H^{\pm},\ Z_H,\ A_H$ (or heavy γ).
- New heavy Higgs particles forming an $SU(2)_L$ triplet: $\phi^o,\ \phi^+,\ \phi^{++}$.

The new quark **T** is a singlet under $SU(2)_L$ up to its small mixing with SM top quarks. Interestingly, the most important divergences are cancelled between the loops of particles with the same statistics. The mass upper limits of the new particles depend on the relative importance of the contribution to the SM Higgs boson mass:

- $m_{\mathbf{T}} < 2$ TeV/c^2 $(\frac{m_{\rm h}}{200\ {\rm GeV}/c^2})^2$
- $M_{\rm W_H} < 6$ TeV/c^2 $(\frac{m_{\rm h}}{200\ {\rm GeV}/c^2})^2$
- $m_\phi < 10$ TeV/c^2

Among all the new particles predicted in this model, **T** is likely to be the least massive and hence likely to be more easily produced at the LHC. The potential of the CMS experiment at the LHC to discover **T** is therefore investigated with limited integrated luminosity of initial years.

Experiments at LEP and Tevatron have searched for new particles beyond the SM and the results are all negative. The paradox is that while trying to eliminate the quadratic divergences in the SM Higgs boson mass *Little Higgs model* predicts existence of particles at TeV scale, but the precision measurements at LEP have put severe constraints on the properties of these particles (Ref. [4]). In general, with reasonable fine-tuning (10%) of the SM Higgs boson mass, the constraints can be accommodated within specific regions of parameter space of the model. Typically the requirement of cancellation of the counter-contribution from the SM top quark by **T** keeps its mass to a moderate value. We are thus motivated to use a value of m_T = 1 TeV/c^2 (Ref. [5]).

2 Phenomenology at hadron colliders

The phenomenology of the *Littlest Higgs* model at the colliders is discussed in Ref. [6]. The heavy gauge bosons can be produced at the LHC via Drell-Yan type processes. The heavy quark **T** can be produced in pairs via QCD (gluon-gluon fusion) in a model-independent way, $gg \to T\bar{T}$ and $q\bar{q} \to T\bar{T}$; however, the cross section falls off rapidly, with increasing mass.

T can also be singly produced: $q\,b \to q'\,T$, through t-channel fusion process $W^+b \to T$. In this case the cross section, though larger, depends on the parameters of the model, relating the mixing of **T** with the conventional top quark. The tree-level Feynman diagram for the production of single **T** is presented in Fig. 1. The Yukawa couplings of **T**, corresponding to two guage groups are given in terms of two constants (free parameters), λ_1 and λ_2 which should be of same order. The mass, m_T, is dependent on these constants which can have relations $\lambda_1/\lambda_2 = 0.5, 1, 2$. The production cross section at the LHC, as a function of $M_{\rm T}$ and this ratio is given in Fig. 2. Thus, the single **T** production cross section is taken to be 0.192 pb for $M_{\rm T} = 1$ TeV/c^2 and $\lambda_1 = \lambda_2$ (solid line in Fig. 2) or 0.770 pb for $M_{\rm T} = 1$ TeV/c^2 and $\lambda_1 = 2\lambda_2$ (upper dot line in Fig. 2); the rate is much lower for $\lambda_1 = 0.5\lambda_2$ (lower dot line).

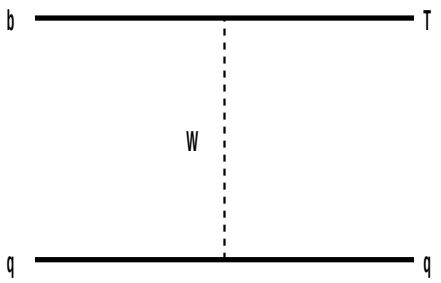

Figure 1: The tree-level Feynman diagram for the production of single, top-like quark (T).

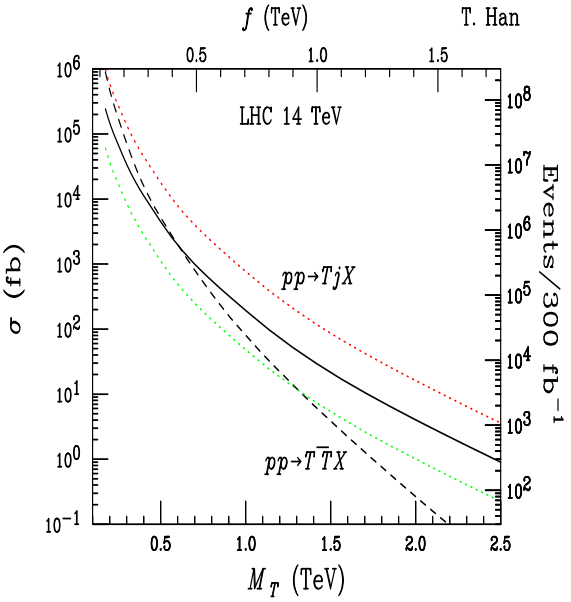

Figure 2: Heavy top-like quark production cross section at the LHC energies as a function of its mass. The dashed line shows the $T\bar{T}$. The solid line shows the single **T** cross section for $\lambda_1 = \lambda_2$ and the dot lines show the single **T** cross section for $\lambda_1 = 2\lambda_2$ (upper line) and for $\lambda_1 = \frac{1}{2}\lambda_2$ (bottom line)

3 Heavy Top Search in CMS

The detection capability and possible discovery of singly-produced **T** are reported in the following sections. The goal of this study is to estimate the viability of this channel for an integrated luminosity of 30 fb^{-1}. The study is performed through the decay channel $\mathbf{T} \to t\,Z$, which has a branching fraction of 25% and is expected to give the clearest signal due to the modes $Z \to e^+e^-$ and $\mu^+\mu^-$ combined with the SM top decay, where all but τ decay modes of W are taken into account ($W \to e\nu_e$ or $\mu\nu_\mu$). The other possible modes $\mathbf{T} \to t\,h$ (with branching fraction of 25%) and $\mathbf{T} \to bW$ (with branching fraction

Table 1: Major background types with their cross section, the expected number of events at luminosity 30 fb^{-1} and the number of events analyzed for this study.

Background	$\sigma\times$ BR (pb)	$N_{\rm expected}$ ($\mathcal{L}$=30 fb^{-1})	$N_{\rm analyzed}$
$\rm t\bar{t} \rightarrow$ leptons	85	2550K	908K
inclusive ZW $\rightarrow$ leptons	2.6	78K	49K
inclusive ZZ $\rightarrow$ leptons	0.16	4.8K	93K
inclusive WW $\rightarrow$ leptons	19.8	549K	93K
Z $\rightarrow \ell\ell$ +jets	161.7	4851K	142K
$\rm Zb\bar{b}$	116	3480K	98K

of 50%) are expected to have more complex final states and much higher SM background events and thus will not be addressed here.

The complete process with the final state considered is $\rm q\,b \rightarrow q'\,T,\ T \rightarrow Zt,\ \ Z \rightarrow \ell^+\ell^-,\ \ t \rightarrow bW,$ $\rm W \rightarrow \ell\nu$. There are three isolated charged leptons, one b jet, and genuine missing transverse energy in the central region of the detector.

3.1 Event Generation and Simulation method

PYTHIA 6.227 (Ref. [7]) was used with subprocess number 83 for $4^{\rm th}$ generation heavy quark production in t-channel process $\rm q_i f_j \rightarrow Q_k f_l$ ($\rm Q_k = \mathbf{T}$). The PYTHIA decay table was modified to treat this particle as a resonance. The CMS framework was used for signal event generation (Ref. [8]) with CTEQ5L as structure function parametrisation. The background events were also generated mostly with PYTHIA.

The major background types with their cross section, the expected number of events at luminosity 30 fb^{-1} and the number of events analyzed are shown in Table. 1. It is impossible to simulate the background channels for full statistics. We have considered inclusive vector-boson pair production as well as inclusive Z production. For $\rm t\bar{t}$ and double Vector Boson productions (*ie.*, WW, WZ, ZZ) the accompanying jet is not very hard in PYTHIA. The production rate for Z+jets and Drell-Yan events is very high ($\sim$ 10 nb). The third lepton may be either from the jet misidentification or due to the initial state gluon radiation in DY events. To save on computing resources we have considered for Z + jets background a specific kinematic region of ($\hat{p}_t$ =75-500 GeV/c) which overlaps with typical transverse momentum of Z in the signal subprocess.

The CMS full detector simulation was performed with OSCAR (Ref. [9]) and event pile-up, corresponding to low luminosity running period of LHC, were taking into account.

3.2 Kinematics at Generator Level of $\rm T \rightarrow Zt,\ Z \rightarrow \ell^+\ell^-$ ($\ell = e, \mu$)

A preliminary study of the kinematics of the signal events, $\rm q\,b \rightarrow q'\,T$, where $\mathbf{T} \rightarrow$ t Z, was performed, at parton level after the event generation using PYTHIA. Fig. 3 shows the typical transverse momentum of **T** and its daughters SM top and Z. The corresponding pseudo-rapidity distributions are plotted in Fig. 4. The source of the initial state b quark is gluon splitting. Being a t-channel process, both the initial and final state quarks have forward/backward directions. In the final state the particles are highly energetic due to the heavy mass involved; the T-decay products as well as particles in the subsequent decay chains are central in the detector.

3.3 Event Reconstruction

A brief description of the reconstruction algorithms for different objects is given below. We have used standard reconstruction software of CMS, ORCA (Ref. [10]), for both physics object and event reconstruction. The jets are reconstructed by the Iterative Cone algorithm with the cone size of 0.5 (Ref. [12])

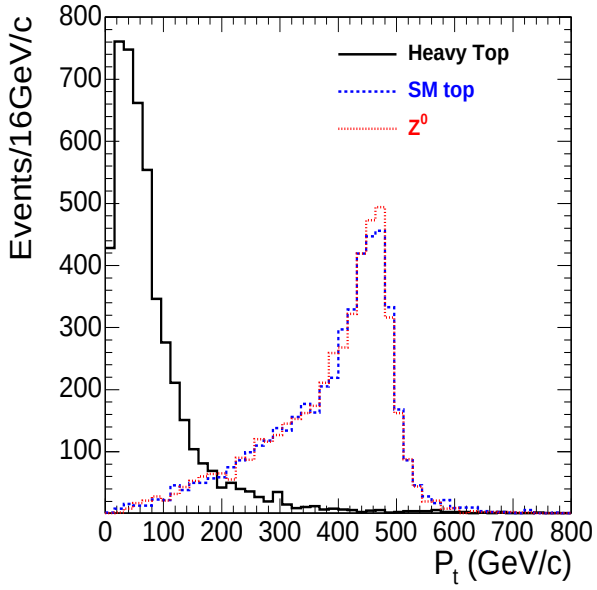

Figure 3: Transverse momentum distributions of the heavy **T** quark(solid), the SM top (dash) and the Z (dot-dash).

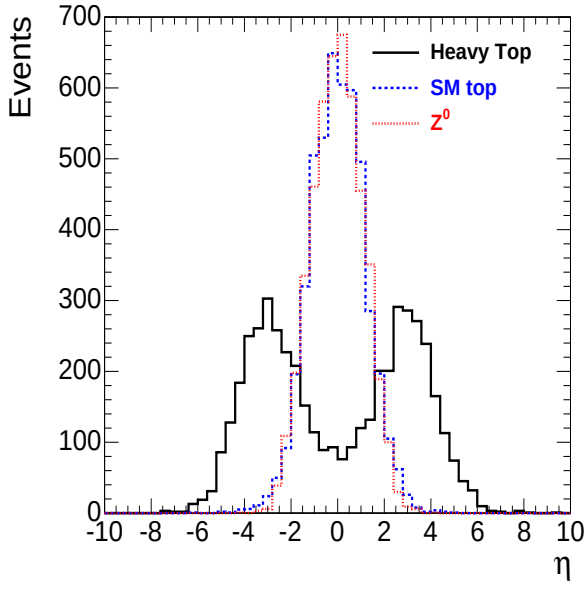

Figure 4: Pseudorapidity distribution of the heavy **T** quark(solid), the SM top (dash) and the Z (dot-dash).

with a seed threshold of energy 1 GeV. For the jet energy calibration the 'gamma + jets' method is used (Ref. [13]). A cut on jets with the minimum transverse energy of 10 GeV is applied during jet reconstruction.

The b-tagging of jets plays a crucial rôle in this study and it is effective up to $|\eta| \leq 2.5$. The signal may be mimicked by the mis-identification of a light quark jet as a b-jet, though such probability is less than about 1% (Ref. [11]). For b-tagging a probability algorithm based on the impact parameter of the tracks is used, as described in Ref. [14].

The missing transverse energy in the event, $\not\!\!E_{\rm T}$, is estimated from the following expression:

$$\vec{\not\!\!E}_{\rm T} = -\sum \vec{E}_T(tower) - \sum (\vec{E}_T^{calib}(jet) - \vec{E}_T^{raw}(jet)) \quad (1)$$

where $\sum \vec{E}_T(tower)$ is the sum of the transverse energy of the calorimeter towers, $\vec{E}_T^{calib}(jet)$ and $\vec{E}_T^{raw}(jet)$ are the transverse energy of calibrated and raw jets respectively. The second summation is over the jets. We have not corrected the $\not\!\!E_{\rm T}$ for the muon momentum. The distribution for the missing transverse energy is plotted in Fig.5; the comparison with the transverse momentum distribution of the true neutrinos (from generator information) show that this $\not\!\!E_{\rm T}$ definition is well-suited for the current analysis.

The electrons and muons are reconstructed by the standard CMS algorithm combining informations from the tracker and ECAL (Ref. [16]) or tracker and muon chamber (Ref. [15]) respectively .

Some additional selections (quality cuts) have to be defined to separate leptons coming from W and Z from fake leptons (e.g. hadrons misidentified) or leptons from b-cascade decays or muons from decays in flight (e.g. $\pi \to \mu$, K $\to \mu$) or electrons from photoconversions. We applied a selection scheme already proposed for the CMS environment (Ref. [16]) which are briefly summarized here:

- the energy deposit of an electron is almost fully contained in electromagnetic calorimeter (ECAL),

while the hadrons tend to leave energy in hadron calorimeter (HCAL). A cut $E_{HCAL}/E_{ECAL} < 0.03$ is applied.

- for electrons, energy in the calorimeter and track momentum have to be almost equal: we choose $E(e)/p(e) > 0.8$.

- the isolation is defined choosing a cone $\Delta R < 0.1$ around the candidate electron or muon track and looking at the other tracks inside it. These tracks are selected if they have $p_T > 0.9$ GeV/c, the number of hits > 4 and are close enough to the candidate track, with $|z(track) - z(candidate)| < 0.4$ and $|T(track) - T(candidate)| < 0.1$, where T and z are the longitudinal and transverse component of distance of the closest approach of the tracks from their origin. The electron or muon candidate track itself is removed from this collection. The p_T sum of the selected tracks is set to be less that 4% of the p_T of the candidate in case of muons or the transverse ECAL energy in case of electron.

- in case of multiple electron tracks pointing to the same EM cluster we select the one with the minimum pseudorapidity distance ($\Delta\eta$) between the electromagnetic cluster barycenter and the extrapolated ECAL track position.

3.4 Event Selection and Results

The reconstructed events are firstly checked if they pass standard CMS-trigger criteria in two consecutive steps level1 (L1) and higher level (HLT). For 'double electron' and 'double muon' topology, the thesholds for lepton transverse momentum at higher level trigger are 17 GeV/c and 7 GeV/c respectively (Ref. [17]). The combined trigger efficiency was evaluated to be 95%. Thus, our main selection including trigger and off-line conditions can be summarized below:

- Events should pass the 'double electron or double muon' L1 and HLT trigger criteria. The p_T distribution of e^+/e^- candidates for signal and the various backgrounds after trigger cuts is shown in Fig. 6. Similar distributions for muon candidates is shown in Fig. 7. For off-line analysis events are accepted for e^+/e^- candidates with $p_T > 20$ GeV/c and μ^+/μ^- candidates with $p_T > 10$ GeV/c.

- The 'same flavour opposite sign dileptons:' e^+e^- and $\mu^+\mu^-$ combinations should have a $p_T > 100$ GeV/c (Fig 8) and a mass ± 10 GeV/c^2 around the nominal Z mass (Fig 9). This is referred to later as *Z criteria*.

- The event should contain a third lepton: if electron, with $p_T > 20$ GeV/c or if muon with $p_T > 15$ GeV/c. To be compatible with a leptonic decay of W this lepton, in combination with missing energy (of nominal value $E_T^{\rm Miss} > 20$ GeV), should have a transverse momentum of $p_T > 60$ GeV/c (Fig. 10) and a transverse mass less than 120 GeV/c^2 (Fig. 11). This is referred to as *W criteria*.

- We allow only one jet with transverse momentum > 30 GeV/c within the tracker acceptance ($|\eta| < 2.5$) satisfying the conditions of a b-jet. The combination of W and the b-jet should have a transverse momentum > 150 GeV/c, as shown in Fig. 12). This condition is referred to as *W + b-jet criteria*.

- The combination of W and b-jet is required to have a mass in the range $110 - 220$ GeV/c^2 (Fig. 13), referred to as *SM top criteria*.

- Finally we apply the *Heavy quark* characteristics: the combination (Z, W, b) should have a mass in the range $(850 - 1150)$ GeV/c^2 since our input mass at generation was 1 TeV/c^2 (Fig. 14).

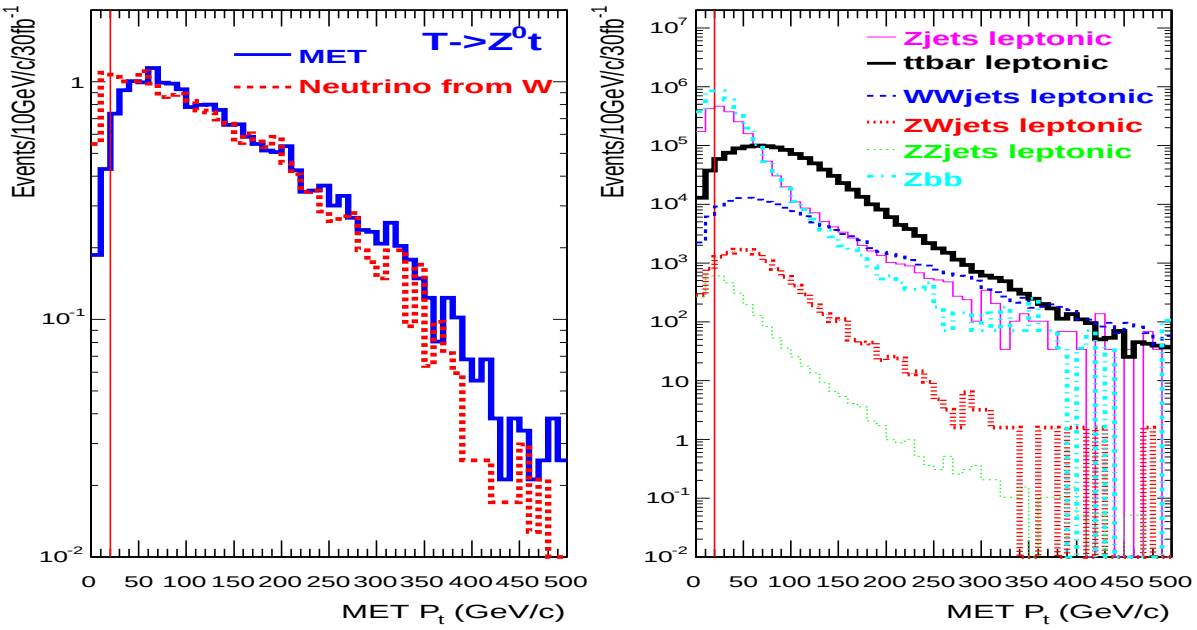

Figure 5: Missing transverse energy distribution for signal (top plot) and background (bottom plot). The vertical line shows the cut value used later in the analysis. The normalization is done for an integrated luminosity of 30 fb^{-1}.

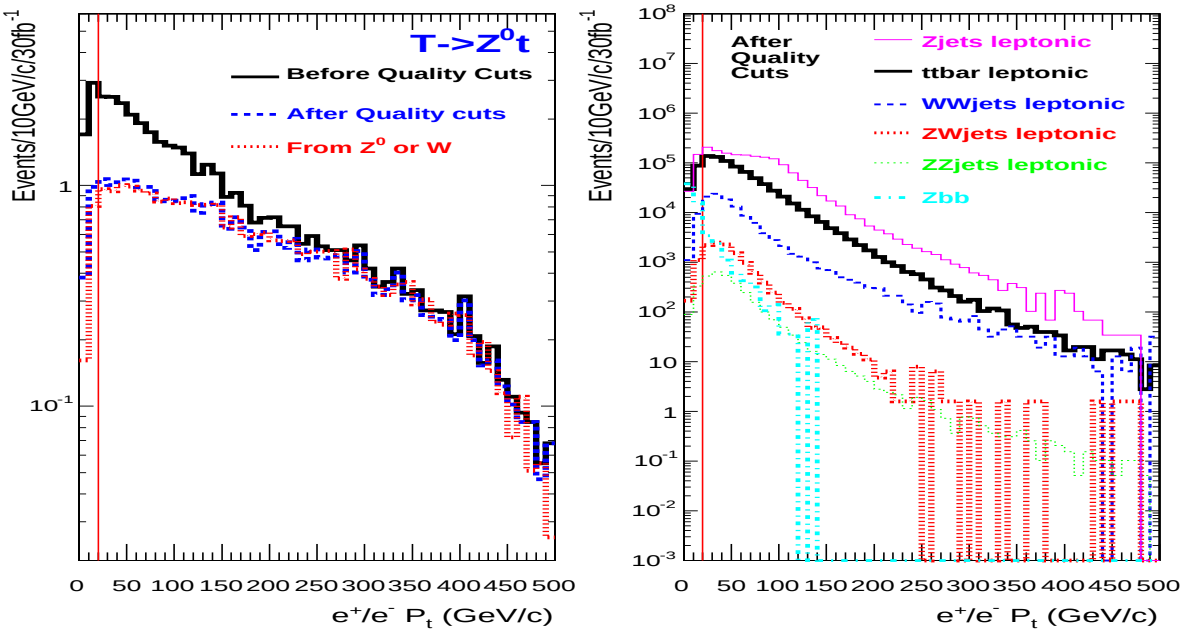

Figure 6: The transverse momentum of e^+/e^- candidates for signal (top plot) and background (bottom plot). The vertical line indicates the offline cut ($P_T > 20$ GeV/c). The normalization is done for an integrated luminosity of 30 fb^{-1}.

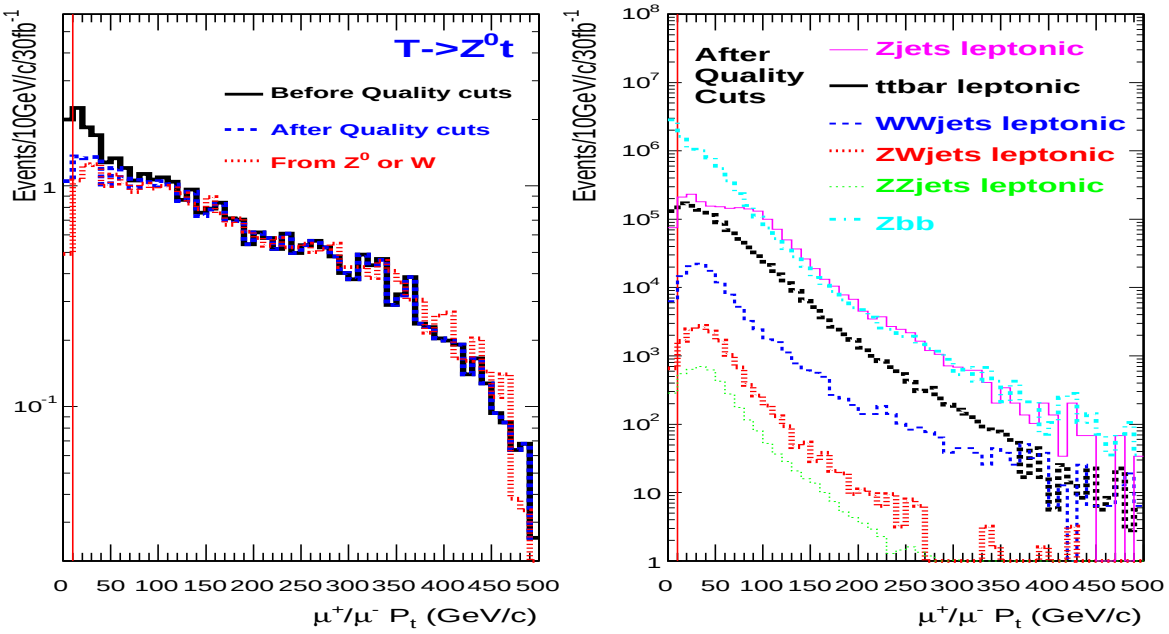

Figure 7: The transverse momentum of μ^+/μ^- candidates for signal (top plot) and background (bottom plot). The vertical line indicates the offline cut ($P_T > 10$ GeV/c). The normalization is done for an integrated luminosity of 30 fb^{-1}.

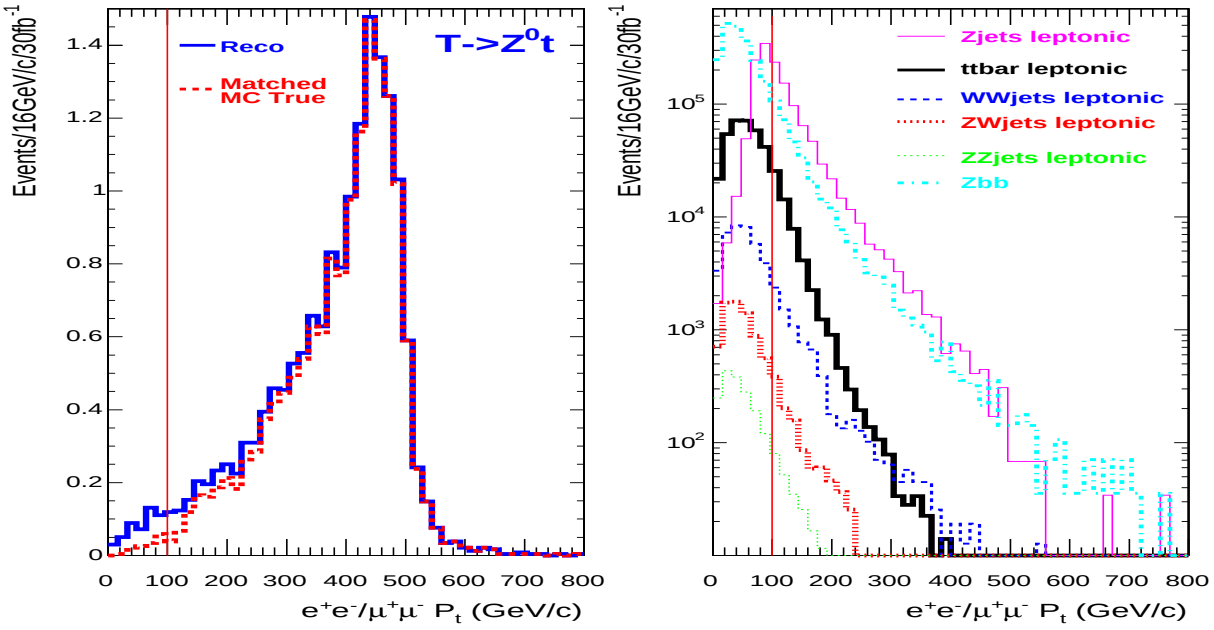

Figure 8: The transverse momentum of the e^+e^- and $\mu^+\mu^-$ combinations for signal (top plot) and background (bottom plot). The vertical line shows the cut value. The normalization is done for an integrated luminosity of 30 fb^{-1}.

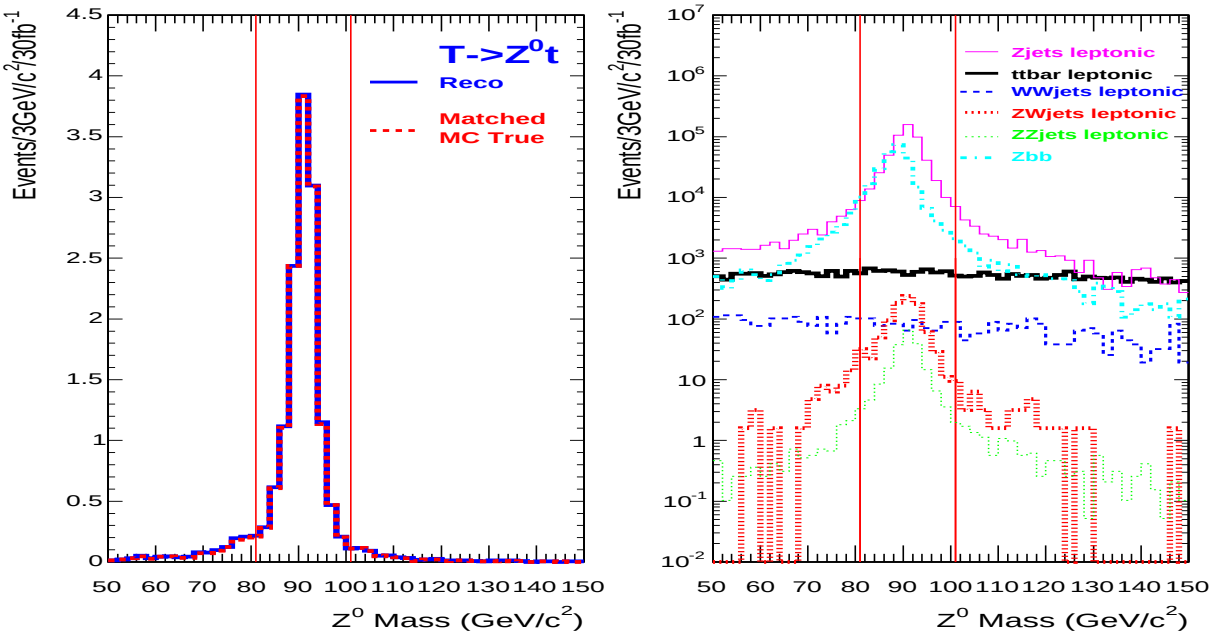

Figure 9: The invariant mass of the e^+e^- and $\mu^+\mu^-$ combinations for signal (top plot) and background (bottom plot). The vertical lines show the cut value.The normalization is done for an integrated luminosity of 30 fb^{-1}.

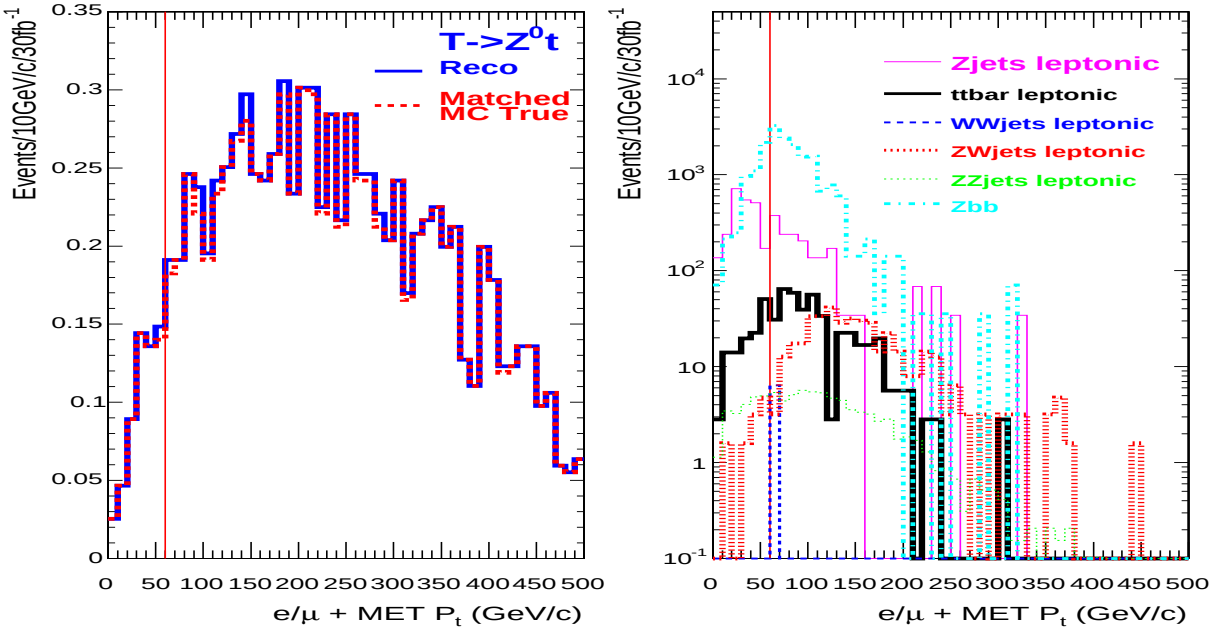

Figure 10: The transverse momentum of the e^+/e^- or μ^+/μ^- and missing energy combinations and b-jet combinations for signal (top plot) and background (bottom plot). The vertical line indicates the cut ($p_T > 60$ GeV/c). The normalization is done for an integrated luminosity of 30 fb^{-1}.

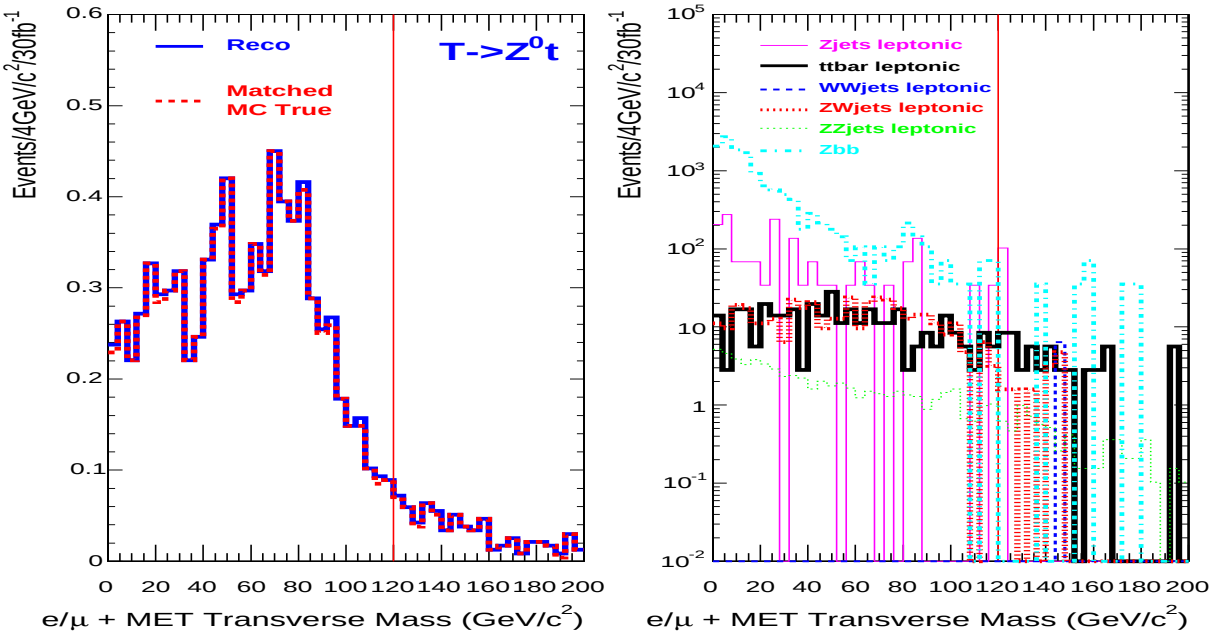

Figure 11: The transverse invariant mass of the e^+/e^- or μ^+/μ^- and the missing energy for signal (top plot) and background (bottom plot). The vertical line indicates the accepted mass region ($M_T < 120$ GeV/c^2) to be considered as W candidates.The normalization is done for an integrated luminosity of 30 fb^{-1}.

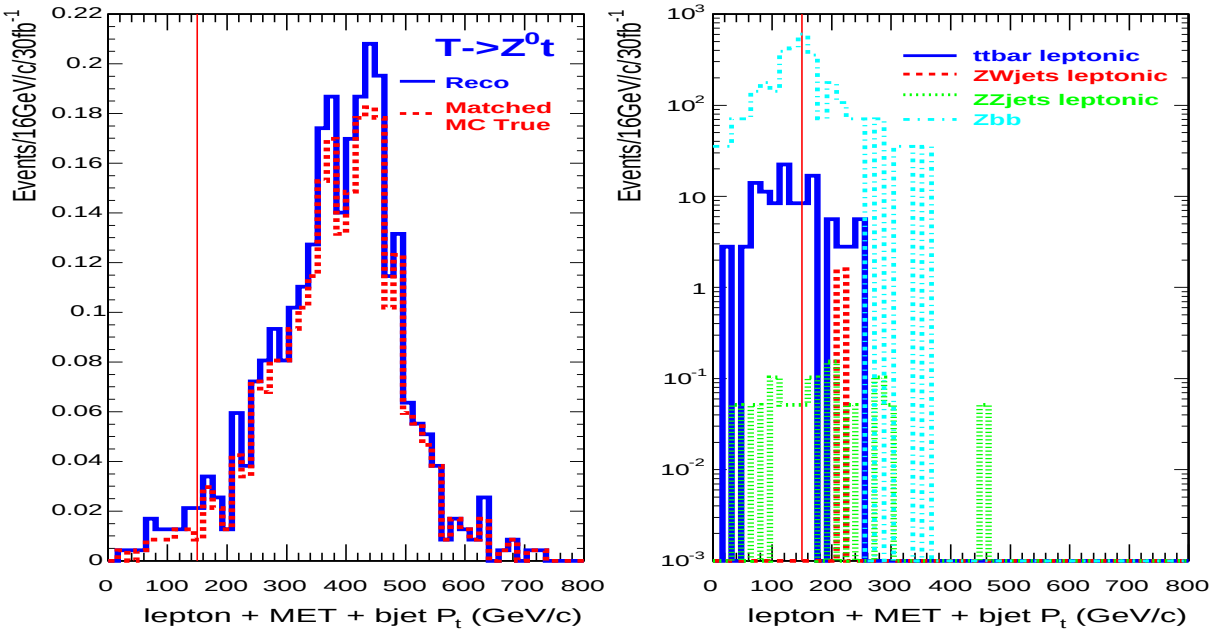

Figure 12: The transverse momentum of the e^+/e^- or μ^+/μ^- and missing energy and bjet combinations for signal (top plot) and background (bottom plot). The vertical line shows the cut value (150 GeV/c). The normalization is done for an integrated luminosity of 30 fb^{-1}.

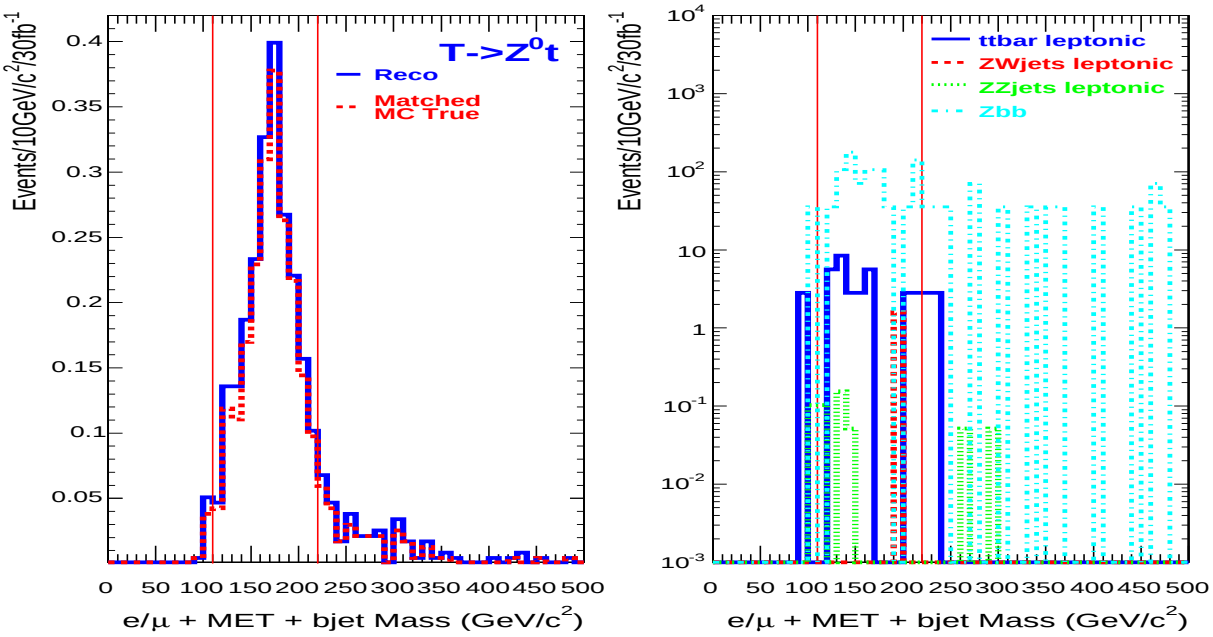

Figure 13: The invariant mass of the e^+/e^- or μ^+/μ^- and missing energy and b-jet combinations for signal (top plot) and background (bottom plot). The vertical lines indicates the accepted mass range (110 GeV/c^2 < $M_{\ell\nu b}$ < 220 GeV/c^2) to be considered as SM top candidates. The normalization is done for an integrated luminosity of 30 fb^{-1}.

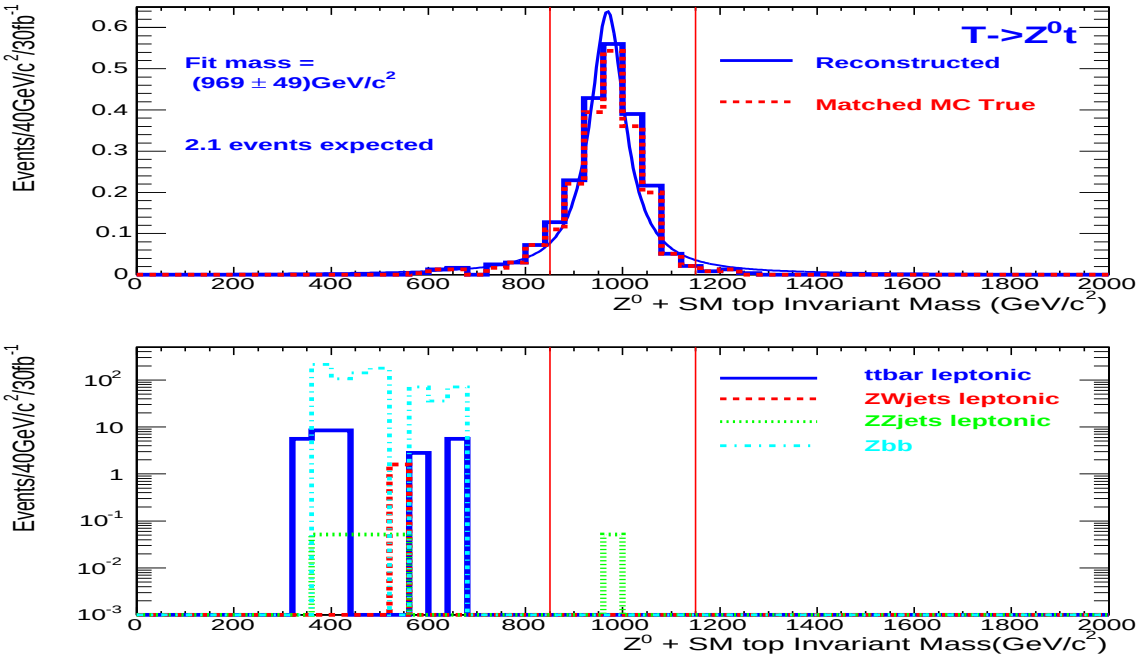

Figure 14: The invariant mass of the Z and SM top combination for signal (top plot) and background (bottom plot). The vertical lines indicate the accepted mass region (850 GeV/c^2 < $M_{\mathrm{Z\ t}}$ < 1150 GeV/c^2) to be considered as heavy top candidates.The normalization is done for an integrated luminosity of 30 fb^{-1}.

Table 2: Efficiency of the selection criteria to the signal and the various backgrounds analyzed. In parentheses are the expected number of events at L = 30 fb $^{-1}$.

Selection	$T \to Zt$ (%)	$t\bar{t} \to$ lept (%)	ZZ (%)	ZW (%)	WW (%)	Z+ jets (%)	$Zb\bar{b}$ (%)
Trigger	95(20.2)	43(1.1M)	59(2.8K)	16(12K)	25(149K)	43(2.1M)	92(3.2M)
Z	63(13.4)	0.24(6.1K)	4.160(197)	1.13(858)	0.14(831)	11(0.5M)	7.4(257K)
W	39(8.3)	0.014(357)	1.120(58)	0.5(390)	0.(0)	0.036(1.7K)	0.39(1.3K)
W + bjet	13(2.8)	0.005(127)	0.020(1)	0.002(1.6)	0.(0)	0.(0)	0.09(3.1K)
SM top	11(2.3)	0.001(25)	0.006(0.3)	0.002(1.6)	0.(0)	0.(0)	0.02(696)
Heavy quark	9.7(2.1)	0.(0)	0.001(0.05)	0.(0.)	0.(0)	0.(0)	0.(0)
$N_{\rm sel}$ (30 fb^{-1})	2.1	0	0.05	0	0	0	0

In Table. 2 we have summarized the efficiency of our selection cuts both on signal and background. The hard cuts applied for signal are effective in removing the backgrounds almost in all cases.

The only SM background which survives all selections is ZZ $\to$ leptonic. So the total number of background events, N_B, is less than one (0.05) event at luminosity 30 fb^{-1}. The total efficiency for the signal selection is $(9.7 \pm 0.4)\%$. Taking into account the single heavy **T** production cross section, 192 fb, (for the case of $\lambda_1 = \lambda_2$) for heavy **T** mass of 1 TeV/c^2 (see Fig. 2) and the various branching ratios: BR(T $\to$ t Z) $= 0.25$, BR(Z $\to e^+e^-,\ \mu^+\mu^-) = 0.067$ and BR(W $\to e\nu,\ \mu\nu) = 0.22$, we can calculate that a signal sample of $N_S = 2.1 \pm 0.1$ events are expected with an integrated luminosity of 30 fb^{-1}.

Since the search is limited by statistics the significance could be calculated from the formula (Ref. [18]):

$$S_{c12} = 2(\sqrt{N_S + N_B} - \sqrt{N_B}) \quad (2)$$

which gives: $S_{stat} = S_{c12} = 2.5$ with a signal-to-background ratio of 41.

4 Systematics

For all experimental sources, shifts and rescaling on the observed objects (leptons, jets and photons) are applied after the reconstruction in a consistent way and their impact on the selection efficiency (ϵ) and the surving number of background events (N_B) is evaluated. Only uncorrelated (or with negligible correlation) sources are included, and fluctations are considered as the maximum shift for the central value without the systematic bias.

Lepton Energy Scale: Due to imperfect knowledge of material in the detector, magnetic field or initial misalignements, estimates of 4-momenta of leptons have an uncertainty. This effect is accounted for by rescaling all reconstructed lepton energies and momenta by a factor ± 0.005. The error in ϵ is found to be 0.4%, whilst the background is not significantly affected.

Jet and Missing Energy Scale: The jet energy scale uncertainty (after 10 fb^{-1} integrated luminosity) is expected to be $\pm 5\%$ for jets with p_T =20 GeV/c and $\pm 2.5\%$ for jets with $p_T > 50$ GeV/c. In the range 20 GeV/$c < p_T < 50$ GeV/c a linear dependence is assumed, as a rough approximation of the true dependence (Ref. [19]). With a $\not{E}_T$ estimated from jet energies, missing energy scale is totally correlated to the Jet Energy Scale and has changed simultaneously by $\pm 5\%$. The error in the ϵ is found to be 1% whilst the background is not significantly affected;

b-tag uncertainty: The b-tag uncertainty is assumed to be 4% after 10 fb^{-1} integrated luminosity (Ref. [20]). Tagging uncertainty variations with p_T and η of jets are below 1% and are neglected. Changing the number of selected b-jets results in a large effect both on ϵ (5%) and on ΔN_B (± 0.15 events).

So the significance taking into account the systematics is given by equation (3) as in Ref. [21]:

$$S_{stat+syst} = S_{stat}\sqrt{\frac{N_{\rm B}}{N_{\rm B} + (\Delta N_B)^2}} \tag{3}$$

Thus, $S_{stat+syst} = 2.5 \times 0.83 = 2.0$.

Thus, the significance of the channel worsens after systematic effects are taken into account. The situation can improve significantly when the signal cross-section is higher as for the choice $\lambda_1/\lambda_2 = 2$.

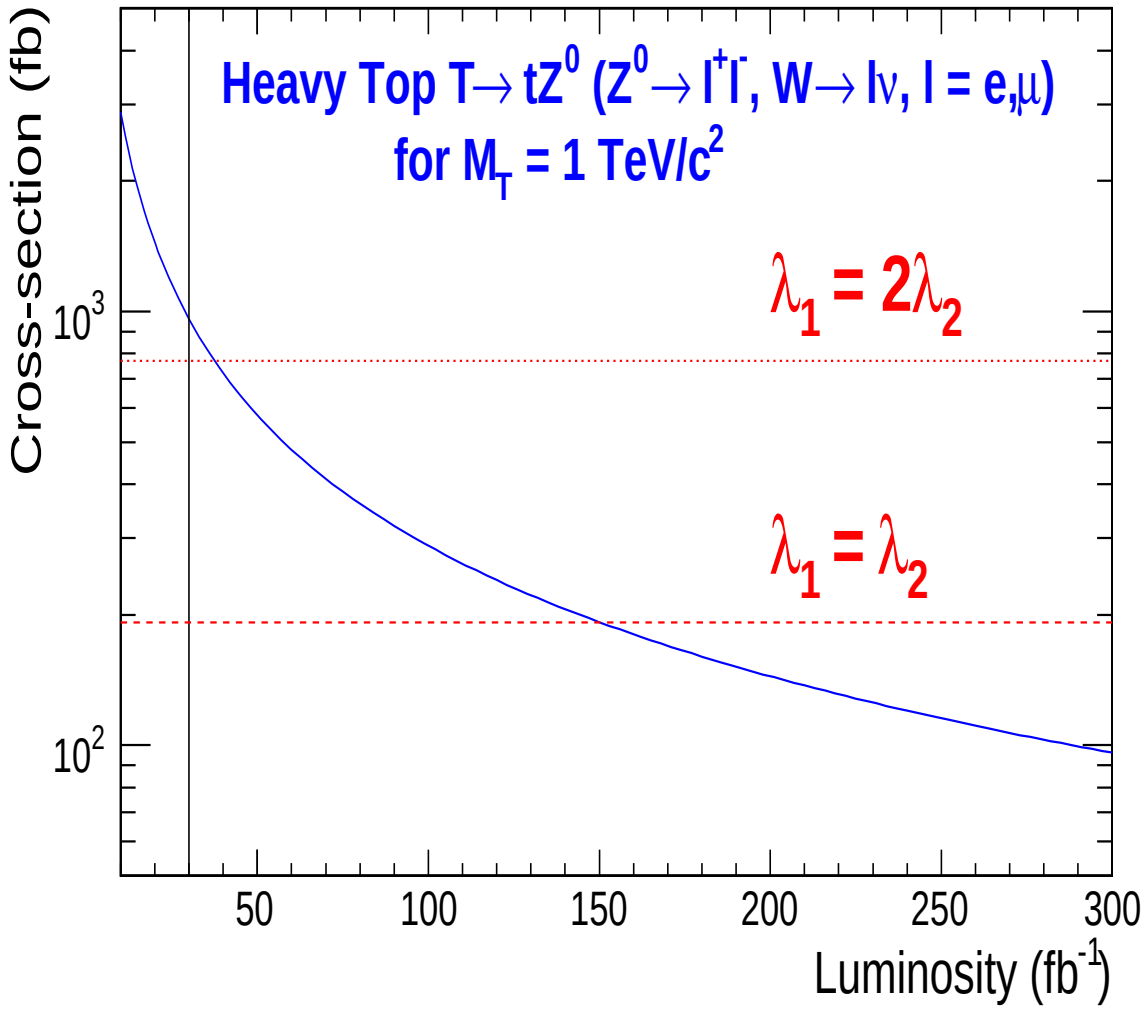

Figure 15: The discovery plot. The curve represents the signal cross-section required as a function of integrated luminosity at LHC, for establishing single production of a heavy quark of mass = 1 TeV/c^2 at 5σ level. The horizontal lines correspond to various choices of λ_1/λ_2. The vertical line corresponds to the luminosity used for this analysis *ie.*, 30 fb $^{-1}$.

5 Conclusion

The *Little Higgs* model predicts the existence of a top-like heavy quark, **T**, in the few TeV/c^2 range. The experimental signature of single **T** production at the LHC was studied with subsequent decays in $\mathbf{T} \to \mathrm{Zt},\ \mathrm{Z} \to \ell^+\ell^-$ where the W from top-quark decays leptonically. After all the selections, we determine, the total signal efficiency to be $(9.7 \pm 0.4)\%$. The main contribution of the background is due to events of type ZZ + jets. The study demonstrates that with an integrated luminosity of 30

fb^{-1}, the discovery potential of the channel $T \rightarrow tZ$, with leptonic decays of Z and W, is rather limited. Fig. 15 shows signal cross-section required as a function of integrated luminosity, for establishing at 5σ level, single production of a heavy quark of mass = 1 TeV/c^2. The luminosity needed for 5σ evidence is estimated to be around 150 fb^{-1} and 40 fb^{-1} respectively for choice of parameters $\lambda_1 = \lambda_2$ and $\lambda_1 = 2\lambda_2$. The vertical line corresponds to the luminosity used for this analysis and demonstrates the inadequacy of statistics for a luminosity of 30 fb^{-1}.

6 Acknowledgements

The authors would like to thank Oliver Buchmueller and Roberto Tenchini for refereeing this note and Maria Spiropulu, Luc Pape and Albert De Roeck for the useful discussions.We also would like to thank the CMS production team for providing the Monte Carlo samples, all the members of CMS who contributed to the development of all software packages used in this study and our home institutes that provided the financial support.

References

[1] http://lepewwg.web.cern.ch/LEPEWWG/

[2] N.Arkani-Hamed, A.G.Cohen and H.Georgi: *JHEP* 0207 (2002) 020.
N.Arkani-Hamed, A.G.Cohen and H.Georgi: *Phys. Lett. B* 513 (2001) 232.
H.Georgi and A.Pais: *Phys.Rev. D* 10 (1974) 539.
D.B.Kaplan, H.Georgi and S. Dimopoulos: *Phys. Lett. B* 136 (1984) 187.

[3] N.Arkani-Hamed, A.G.Cohen, E.Katz and A.E.Nelson: *JHEP* 0207 (2002) 034.
N.Arkani-Hamed, A.G.Cohen, E.Katz, A.E.Nelson, T. Gregoire and J.G.Wacker: *JHEP* 0208 (2002) 021.

[4] C.Csaki, J.Hubisz, G.D.Kribs, P.Meade and J.Terning: arXive: hep-ph/0211124.
J.L.Hewett, F.J.Petriello and T.G. Rizzo: arXive: hep-ph/0211218.

[5] S.Chang: arXive: hep-ph/0306034.
D.E.Kaplan and M.Schmaltz: arXive: hep-ph/0302049.

[6] Tao Han, Heather E. Logan, Bob McElrath, and Lian-Tao Wang: Phenomenology of the Little Higgs model; *Phys. Rev.D*, 67 (2003) 095004.

[7] T.Sjostrand, L.Lonnblad and S.Mrenna, http://www.thep.lu.se/∼torbjorn/Pythia.html

[8] V. Karimaki, D.Bourilkov, A. Nikitenko, S. Slabospitsky, http://cmsdoc.cern.ch/cmsoo/projects/CMKIN/
Physics TDR Vol I, Section 2.5.1

[9] CMS Coll., *Object oriented Simulation for CMS Analysis and Reconstruction*, Physics TDR Vol.I, Section 2.5.2,
OSCAR home page: http://cmsdoc.cern.ch/OSCAR/

[10] CMS Coll., *Object-oriented Reconstruction for CMS Analysis*, Physics TDR Vol.I, Section 2.5.4,
ORCA home page: http://cmsdoc.cern.ch/ORCA/

[11] CMS Coll, Physics TDR Vol.I, Section 12.2.5

[12] CMS Coll., Physics TDR Vol.I, Section 11.2.1.

[13] CMS Coll., Physics TDR Vol.I, Section 11.6.3.

[14] CMS Coll., Physics TDR Vol.I, Section 12.2.2.

[15] CMS Coll., Physics TDR Vol.I, Section 9.1.2.

[16] CMS Coll., Physics TDR Vol.I, Section 10.4.

[17] CMS Collaboration, The Data Acquisition and High-Level Trigger Project, Technical Design Report, CERN/LHCC 2002-26, CMS TDR 6.2, 2002.

[18] V. Bartsch, G. Quast, *Expected signal observability at future experiments*, CMS NOTE-2005/004

[19] CMS Coll., Physics TDR Vol.I, Section 11.6.5.

[20] S.Lowette, J.D'Hondt, J. Heyninck, *Offline Calibration of b-Jet Identification Efficiencies*,CMS NOTE 2006/013

[21] http://cmsdoc.cern.ch/ bityukov